Eur. J. Mineral.
2007, **19**, 399–409

Two new structure types: $KFe_3(AsO_4)_2(HAsO_4)_2$ and $K(H_2O)M^{3+}(H_{1.5}AsO_4)_2(H_2AsO_4)$($M^{3+}$ = Fe, Ga, In) – synthesis, crystal structure and spectroscopy

KAROLINA SCHWENDTNER* and UWE KOLITSCH

Institut für Mineralogie und Kristallographie, Universität Wien, Althanstr. 14, 1090 Wien, Austria
*Corresponding author, e-mail: karolina.schwendtner@univie.ac.at

Abstract: The new arsenates $KFe_3(AsO_4)_2(HAsO_4)_2$ ($C2/c$; Z = 4; a = 18.975(4), b = 6.5850(13), c = 10.955(2) Å, β = 100.42(3)°, V = 1346.3(5) Å^3) and $K(H_2O)M^{3+}(H_{1.5}AsO_4)_2(H_2AsO_4)$ ($P2/n$; Z = 2; a = 4.700(1), 4.641(1), 4.798(10); b = 8.712(2), 8.696(2), 8.832(2); c = 13.828(3), 13.772(3), 13.971(3) Å; β = 94.86(3), 94.71(3), 94.68(3)°; V = 564.2(2), 553.9(2), 590.1(2) Å^3 for M^{3+} = Fe, Ga, In, respectively), were synthesized hydrothermally in Teflon-lined stainless steel autoclaves (493 K, 7–9 d, pH $\leqslant$ 1) from mixtures containing $M_2^{3+}O_3$, $M_2^{1+}CO_3$, $H_5As_3O_{10}$ and distilled water. Single-crystal structure determination (MoKα X-radiation, CCD area detector, 293 K, $R1(F)$ = 0.027–0.056) revealed that $KFe_3(AsO_4)_2(HAsO_4)_2$ represents a novel sheet structure-type, containing shared edges between AsO_4 tetrahedra and FeO_6 octahedra, whereas $K(H_2O)M^{3+}(H_{1.5}AsO_4)_2(H_2AsO_4)$ is a novel chain structure-type consisting of decorated kröhnkite-type (octahedral-tetrahedral) chains with water molecules and K atoms in-between. Structural relationships to related compounds are discussed in detail for both types.

Supplementary SEM and Raman-spectroscopic data are presented. The two new K-Fe^{3+}-arsenate compounds may occur in strongly acidic environments in nature.

Key-words: potassium-iron-arsenate, crystal structure, Raman spectroscopy, $KFe_3(AsO_4)_2(HAsO_4)_2$, $K(H_2O)M^{3+}(H_{1.5}AsO_4)_2(H_2AsO_4)$.

Introduction

Potassium, iron and, to a lesser extent, arsenic are abundant elements in the Earth's crust, and it is not surprising that there are ten ferric iron arsenate minerals known. Interestingly though, among these is only one K-Fe^{3+}-arsenate, *i.e.* pharmacosiderite, $KFe_4(AsO_4)_3(OH)_6 \cdot 6\text{–}7H_2O$ (Takano *et al.*, 1971; Zemann, 1947; 1948; 1959). In comparison, there are also ten ferric iron phosphate minerals known to date, but the K-Fe^{3+}-phosphate minerals are considerably more abundant than corresponding arsenates. The phosphates comprise the four species gengenbachite [$KFe_3((H_2PO_4)(H_2PO_4)_2)_2 \cdot 6H_2O$] (Walenta & Theye, 2004; 2005), haigerachite [$KFe_3(H_2PO_4)_6(HPO_4)_2 \cdot 4H_2O$] (Anisimova *et al.*, 1997; Waerstad & Frazier, 1987; Walenta & Theye, 1999), leucophosphite [$KFe_2(PO_4)_2(OH) \cdot 2H_2O$] (Moore, 1972) and meurigite [$KFe_7(PO_4)_5(OH)_7 \cdot 8H_2O$] (Birch *et al.*, 1996; Kolitsch, 1999). The first two of these represent highly acidic minerals. Synthetic K-Fe^{3+}-arsenates are similarly scarce, only $K_2Fe_2O(AsO_4)_2$ (Chang *et al.*, 1997) and the recently published $K_3Fe_3(AsO_4)_4$ (Ouerfelli *et al.*, 2005) have been described so far.

As part of a detailed ongoing study of synthetic compounds in the system M^{1+}-M^{3+}-As-O-H (M^{1+} = Li, Na, K, Rb, Cs, Ag, Tl, NH_4, H_3O; M^{3+} = Al, Ga, In, Sc, Cr, Fe), which has already lead to numerous interesting results (Baran *et al.*, 2006a,b; Kolitsch, 2004; Kolitsch & Schwendtner, 2004; 2005; Schwendtner, 2006; Schwendtner & Kolitsch, 2004a,b; 2005a,b,c; 2007a,b; Schwendtner *et al.*, 2006a,b,c), we would like to extend this knowledge and present the intriguing and novel crystal structures of two new synthetic K-Fe^{3+}-arsenate compounds, that may also exist as minerals in nature, as well as two isotypic K-Ga and K-In members.

Experimental

Synthesis

The four title compounds were synthesized under mild hydrothermal conditions in Teflon-lined stainless steel autoclaves at 493 K under autogeneous pressure. The autoclaves were filled to about 60–80 % of their inner volume and were then heated to 493 K, kept at this temperature for 7–9 days, and slowly cooled to room temperature overnight. The reaction products were washed thoroughly with distilled water, filtered, and slowly dried at room temperature.

0935-1221/07/0019-1726 $ 4.95

DOI: 10.1127/0935-1221/2007/0019-1726

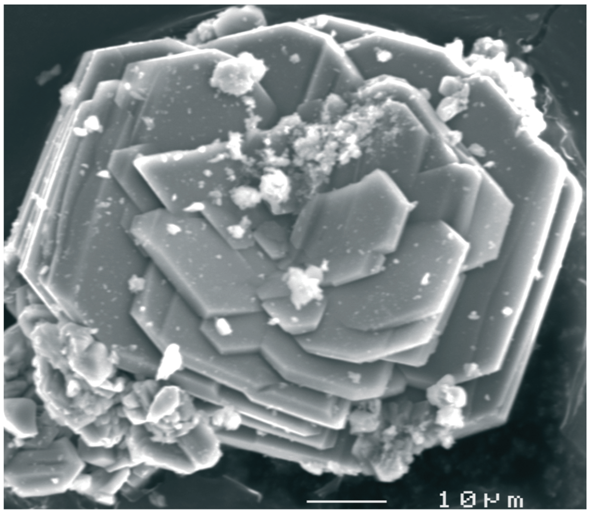

Fig. 1. SEM image of tabular $KFe_3(AsO_4)_2(HAsO_4)_2$ crystals intergrown to form a rosette-like aggregate.

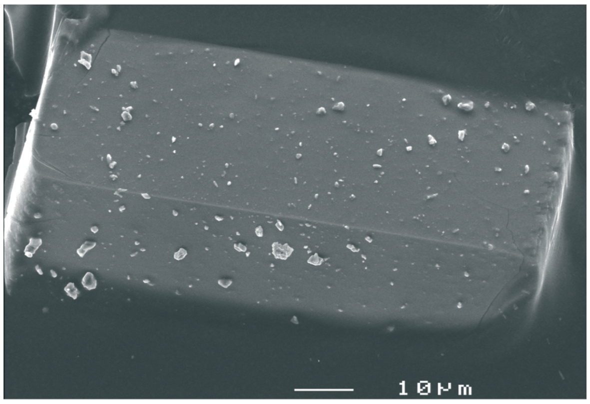

Fig. 2. SEM image of a prismatic $K(H_2O)Fe(H_{1.5}AsO_4)_2(H_2AsO_4)$ crystal.

Tiny pale yellowish green, octagonal to pseudohexagonal platelets of $KFe_3(AsO_4)_2(HAsO_4)_2$ (I) (Fig. 1) and small, colourless prisms of $K(H_2O)Fe(H_{1.5}AsO_4)_2(H_2AsO_4)$ (II) (Fig. 2) were prepared from a mixture of K_2CO_3 (Merck, > 99.5 %), Fe_2O_3 (STREM Chemicals, 99.8 %), $H_5As_3O_{10}$ (Alfa, 99.9 %), and distilled water (run time 9 d). Initial and final pH values were 1 and 0.5, respectively. The yield was about 5 vol.-% of compound I and 95 vol.-% of compound II. Large, colourless, acicular prisms of $K(H_2O)Ga(H_{1.5}AsO_4)_2(H_2AsO_4)$ (III) (Fig. 3) were grown from a mixture of K_2CO_3, Ga_2O_3 (Chempur, 99.99 %), $H_5As_3O_{10}$, and distilled water (run time 7 d). Initial and final pH values were about 1 and 0.5, respectively (yield > 98 vol.-%, accompanied by very few grains of $GaAsO_4$). $K(H_2O)In(H_{1.5}AsO_4)_2(H_2AsO_4)$ (IV) formed colourless, grainy crystals of monoclinic appearance, and was grown from a mixture of K_2CO_3, In_2O_3 (Chempur, 99.9 %), $H_5As_3O_{10}$ and distilled water, with initial and final pH values of about 1 and 1, respectively. The reaction product was only present in very minor amounts, whereas the largest quantity (> 95 vol.-%) of the reaction product was a new $KInAs_2O_7$ compound, isotypic to $TlInAs_2O_7$ (Schwendtner, 2006).

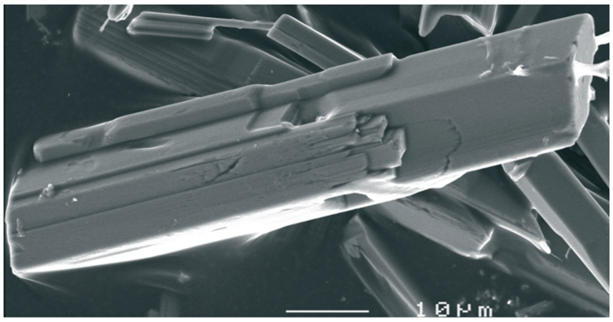

Fig. 3. SEM image of prismatic crystals of $K(H_2O)Ga(H_{1.5}AsO_4)_2(H_2AsO_4)$.

X-ray diffraction experiments and crystal structure solution

Several crystals of each of the three compounds were selected for single-crystal studies with a Nonius KappaCCD single-crystal four-circle X-ray diffractometer (Mo tube, graphite monochromator, CCD area detector), equipped with a 300 µm diameter capillary-optics collimator to provide increased resolution. A complete sphere of reciprocal space was measured at room temperature for a suitable crystal of each compound (see Table 1 for details). The intensity data were processed with the Nonius program suite DENZO-SMN (Otwinowski & Minor, 1997) and corrected for Lorentz, polarization, and background effects and, by the multi-scan method (Otwinowski *et al.*, 2003; Otwinowski & Minor, 1997), for absorption. The crystal structure of compound I was solved in $C2/c$, those of compounds II, III and IV were solved in $P2/n$ by direct methods using SHELXS-97 (Sheldrick, 1997b) and subsequent Fourier and difference Fourier syntheses, followed by anisotropic full-matrix least-squares refinements on F^2 using SHELXL-97 (Sheldrick, 1997a) (Table 1). The model obtained for $K(H_2O)Ga(H_{1.5}AsO_4)_2(H_2AsO_4)$ was used as a starting model for the refinement of isotypic compounds II and IV. A total of 54 reflections most strongly affected by the presence of apparently merohedral twinning ($F_o \gg F_c$, no split reflection spots were observed; twin law could not be identified), were omitted from the dataset of $K(H_2O)In(H_{1.5}AsO_4)_2(H_2AsO_4)$.

The measured crystals of I, II and III were not twinned. The last step of refinement gave the final residuals $R1(F)$ = 0.027, 0.031, 0.028 and 0.056 for I, II, III and IV, respectively (Table 1). All H atoms of the four compounds could be located from the Fourier difference maps, but all O-H lengths had to be restrained; furthermore, the position of two of the four H atoms in compound II had to be fixed. Compounds I, II and III do not show any distinct residual electron densities > |1.5| e/Å^3; compound IV, however, affected by twinning, shows larger electron densities (–2.95 to 2.14 e/Å^3) close to the In and K positions, respectively. The final atomic positions and equivalent isotropic displacement parameters are given in Tables 2a and b, selected

Table 1. Crystal data, data collection information and refinement details for compounds I, II, III and IV.

	$KFe_3(AsO_4)_2(HAsO_4)_2$	$K(H_2O)Fe(H_{1.5}AsO_4)_2(H_2AsO_4)$	$K(H_2O)Ga(H_{1.5}AsO_4)_2(H_2AsO_4)$	$K(H_2O)In(H_{1.5}AsO_4)_2(H_2AsO_4)$
Crystal data				
M_r	764.35	534.77	548.64	593.74
Space group	$C2/c$ (No. 15)	$P2/n$ (No. 13)	$P2/n$ (No. 13)	$P2/n$ (No. 13)
T (K)	293(2)	293(2)	293(2)	293(2)
a (Å)	18.975(4)	4.700(1)	4.641(1)	4.798(10)
b (Å)	6.5850(13)	8.712(2)	8.696(2)	8.832(2)
c (Å)	10.955(2)	13.828(3)	13.772(3)	13.971(3)
β (°)	100.42(3)	94.86(3)	94.71(3)	94.68(3)
V (Å^3)	1346.3(5)	564.2(2)	553.9(2)	590.1(2)
Z	4	2	2	2
D_x (Mg m^{-3})	3.771	3.148	3.289	3.342
μ (mm^{-1})	13.35	10.50	11.82	10.77
Crystal size (mm)	0.08 × 0.05 × 0.03	0.08 × 0.03 × 0.02	0.08 × 0.02 × 0.02	0.05 × 0.03 × 0.03
Data collection				
T_{min}	0.415	0.487	0.452	0.615
T_{max}	0.690	0.817	0.798	0.738
No. of measured, independent and observed reflections	3758, 1959, 1842	3202, 1652, 1368	3126, 1614, 1235	4964, 2549, 2362
Criterion for observed reflections	$I > 2\sigma(I)$	$I > 2\sigma(I)$	$I > 2\sigma(I)$	$I > 2\sigma(I)$
R_{int}	0.019	0.023	0.032	0.018
θ_{max} (°)	30.0	30.0	30.0	35.0
h =	–26 → 26	–6 → 6	–6 → 6	–7 → 7
k =	–9 → 9	–12 → 12	–12 → 12	–14 → 14
l =	–15 → 15	–19 → 19	–19 → 19	–22 → 22
Refinement				
Refinement on	F^2	F^2	F^2	F^2
$R[F^2 > 2\sigma(F^2)]$, $wR(F^2)$	0.027, 0.072	0.031, 0.083	0.028, 0.065	0.056, 0.134
GoF	1.11	1.09	1.03	1.16
No. of reflections	1959 reflections	1652 reflections	1614 reflections	2495 reflections
No. of parameters	116	99	105	105
Weighting scheme	Calculated $w = 1/[\sigma^2(F_o^2) + (0.0381P)^2 + 9.0119P]$ where $P = (F_o^2 + 2F_c^2)/3$	Calculated $w = 1/[\sigma^2(F_o^2) + (0.039P)^2 + 1.6P]$ where $P = (F_o^2 + 2F_c^2)/3$	Calculated $w = 1/[\sigma^2(F_o^2)+ (0.0329P)^2 + 0.1216P]$ where $P = (F_o^2 + 2F_c^2)/3$	Calculated $w = 1/[\sigma^2(F_o^2) + (0.029P)^2+14.6P]$ where $P = (F_o^2 + 2F_c^2)/3$
$(\Delta/\sigma)_{max}$	0.001	0.001	< 0.0001	0.003
$\Delta\rho_{max}$, $\Delta\rho_{min}$ (e Å^{-3})	1.31, –1.31	0.78, –1.06	0.84, –0.74	2.14, –2.95
Extinction coefficient	0.00064(11)	0.0038(11)	0.0027(7)	0.0040(8)

bond lengths and calculated bond valences are presented in Tables 3a and b. Lists of observed and calculated structure factors are available from the authors, as are the anisotropic displacement parameters, which will also be deposited at the EJM.

SEM analysis

Qualitative SEM analyses were conducted using a JEOL JSM 6400 scanning electron microscope with a tungsten hairpin filament. Several crystals of the samples were mounted onto the sample holder with an adhesive carbon foil and carbon-coated. Chemical analyses showed that no impurities were present within detection limits. Secondary electron images were acquired using 10 kV acceleration voltage and a working distance of 16 mm.

Raman spectroscopy

Raman spectra were measured with a notch filter-based Renishaw RM 1000 Raman spectrometer in the spectral range from 4000 to 200 cm^{-1}. The 632 nm laser lines were focused with a 50/0.75 objective on the surfaces of several single crystals of the compounds. The resolution of the system (*i.e.*, the instrument function) was 5 cm^{-1}, the wavenumber accuracy was ~ 1 cm^{-1} (both calibrated with

Table 2a. Atomic positions and equivalent isotropic displacement parameters of $KFe_3(AsO_4)_2(HAsO_4)_2$.

Atom	*x*	*y*	*z*	$U_{\text{eqiv}}/U_{\text{iso}}$
As1	0.077667(17)	0.66239(5)	0.44770(3)	0.00828(10)
As2	0.302535(17)	0.48144(5)	0.27033(3)	0.00790(10)
Fe1	0.25	0.75	0.50	0.00839(14)
Fe2	0.14899(2)	0.48042(7)	0.22501(4)	0.00839(12)
K1	0.0	0.16102(17)	0.25	0.0228(3)
O1	0.07989(14)	0.4942(4)	0.3347(2)	0.0147(5)
O2	0.14863(12)	0.8167(4)	0.4652(2)	0.0110(4)
O3	0.07116(13)	0.5440(4)	0.5802(2)	0.0133(5)
O4(OH)	0.00658(13)	0.8266(4)	0.4090(3)	0.0146(5)
O5	0.35359(13)	0.6794(3)	0.2527(2)	0.0122(5)
O6	0.35353(13)	0.2790(4)	0.3129(2)	0.0124(4)
O7	0.24002(13)	0.5260(3)	0.3637(2)	0.0098(4)
O8	0.23771(12)	0.4425(4)	0.1395(2)	0.0099(4)
H	–0.0364(18)	0.772(9)	0.405(6)	0.05(2)

Table 2b. Atomic positions and equivalent isotropic displacement parameters of $K(H_2O)Fe(H_{1.5}AsO_4)_2(H_2AsO_4)$, $K(H_2O)Ga(H_{1.5}AsO_4)_2(H_2AsO_4)$ and $K(H_2O)In(H_{1.5}AsO_4)_2(H_2AsO_4)$, in line one, two and three, respectively.

Atom	*x*	*y*	*z*	$U_{\text{eqiv}}/U_{\text{iso}}$
K	0.6183(7)	0.9948(3)	0.0091(2)	0.0469(8)
	0.6221(5)	0.9948(3)	0.00933(14)	0.0402(6)
	0.6556(10)	0.9940(4)	0.0081(3)	0.0363(8)
O7(H_2O)	0.75	0.3474(5)	0.25	0.0248(10)
	0.75	0.3416(5)	0.25	0.0223(8)
	0.75	0.3551(8)	0.25	0.0226(13)
Fe	0.75	0.77744(10)	0.25	0.0163(2)
Ga	0.75	0.77461(7)	0.25	0.01229(14)
In	0.75	0.78143(7)	0.25	0.01728(15)
As1	0.20590(8)	0.65359(5)	0.10111(3)	0.01445(14)
	0.20831(7)	0.65344(4)	0.10342(2)	0.01268(12)
	0.20417(12)	0.65205(7)	0.09643(4)	0.01291(14)
As2	0.25	1.03815(7)	0.25	0.01560(17)
	0.25	1.03104(6)	0.25	0.01297(14)
	0.25	1.05180(10)	0.25	0.01479(18)
O1	–0.0235(6)	0.6161(3)	0.1840(2)	0.0180(6)
	–0.0245(5)	0.6144(3)	0.18641(17)	0.0151(5)
	–0.0171(10)	0.6144(5)	0.1794(4)	0.0201(9)
O2	0.4726(6)	0.7755(4)	0.1327(2)	0.0178(6)
	0.4767(5)	0.7766(3)	0.13442(17)	0.0152(5)
	0.4621(9)	0.7744(6)	0.1263(3)	0.0181(8)
O3(OH)	0.3265(7)	0.4832(4)	0.0636(2)	0.0234(7)
	0.3294(6)	0.4830(3)	0.0651(2)	0.0209(6)
	0.3255(10)	0.4824(6)	0.0607(4)	0.0218(10)
O4(OH)	0.0411(8)	0.7457(4)	0.0017(2)	0.0264(7)
	0.0413(6)	0.7449(3)	0.00288(19)	0.0236(6)
	0.0376(11)	0.7436(7)	–0.0013(4)	0.0245(10)
O5	–0.0200(6)	0.9440(3)	0.1916(2)	0.0178(6)
	–0.0236(5)	0.9376(3)	0.19101(17)	0.0144(5)
	–0.0109(10)	0.9577(6)	0.1908(4)	0.0194(9)
O6(OH)	0.1328(8)	1.1558(4)	0.3381(3)	0.0263(7)
	0.1345(6)	1.1499(3)	0.33841(19)	0.0228(6)
	0.1270(12)	1.1658(6)	0.3378(4)	0.0273(11)
H1	0.008(10)	1.230(5)	0.322(4)	0.035(17)
	–0.009(11)	1.212(7)	0.317(5)	0.10(3)
	–0.053(8)	1.183(14)	0.319(9)	0.04(3)
H2	–0.058(11)	0.668(5)	–0.026(4)	0.026(15)
	–0.076(11)	0.675(5)	–0.026(4)	0.08(2)
	–0.122(13)	0.720(12)	–0.037(7)	0.03(3)
H3*	0.8227	0.4136	0.2072	0.06(2)
	0.842(9)	0.407(4)	0.217(3)	0.034(14)
	0.872(16)	0.405(10)	0.215(6)	0.02(2)
H4*	0.4578	0.5049	0.0280	0.05(4)
	0.464(15)	0.504(11)	0.024(5)	0.02(2)
	0.43(4)	0.49(3)	0.010(9)	0.020**

* Coordinates fixed; ** U_{iso} fixed.

the Rayleigh line and the 520.5 cm^{-1} line of a Si standard). The sample spectra were acquired with a nominal exposure time of 15 s.

Results and discussion

Description of the crystal structure of $KFe_3(AsO_4)_2(HAsO_4)_2$

$KFe_3(AsO_4)_2(HAsO_4)_2$ represents a novel layer-structure type (*C*2/*c*), containing 14 atoms in the asymmetric unit (Fig. 4). Both of the two As atoms, all O atoms and the H atom lie on general positions, just like one of the two Fe atoms. The Fe1 and the K atom lie on the centre of symmetry and the two-fold axis, respectively. The Fe atoms are in octahedral coordination (⟨Fe1-O⟩ = 2.019, ⟨Fe2-O⟩ = 2.016 Å). The main building unit in the structure is a $Fe_2As_2O_{15}$-group (Fig. 4), consisting of corner- and edge-sharing AsO_4 and FeO_6 polyhedra. These groups are connected via bridging O atoms to (100) layers which are in turn linked to each other through medium-weak bifurcated hydrogen bonds (D···A = 2.865(4), 2.921(3) Å) (Table 5). The 8-coordinated K atoms lie between these layers.

All bond-valence sums (BVSs), calculated without the contribution of the H-bonds, agree quite well with the expected values (Table 3). The O atom with the lowest BVS (O4, 1.29 valence units (v.u.)) acts as donor of the hydrogen bond; the O atom with the second lowest BVS (O6, 1.83 v.u.) is the acceptor of the strongest H-bond. The bond lengths of both AsO_4-tetrahedra vary quite largely due to their different coordination environments (As1-O = 1.667(2)–1.721(2) Å; As2-O = 1.656(2)–1.730(2) Å): As1 has one elongated bond to OH, whereas As2 has two short bonds and two extremely lengthened bonds to the two O atoms of the shared edge (O7-O8, compare Fig. 4) with the $Fe2O_6$ octahedra. The shared edge between tetrahedra and octahedra, which is rather rare (see next section for discussion) has a major influence, as is reflected in the very large As-O distances to the two shared O atoms (1.725(2),

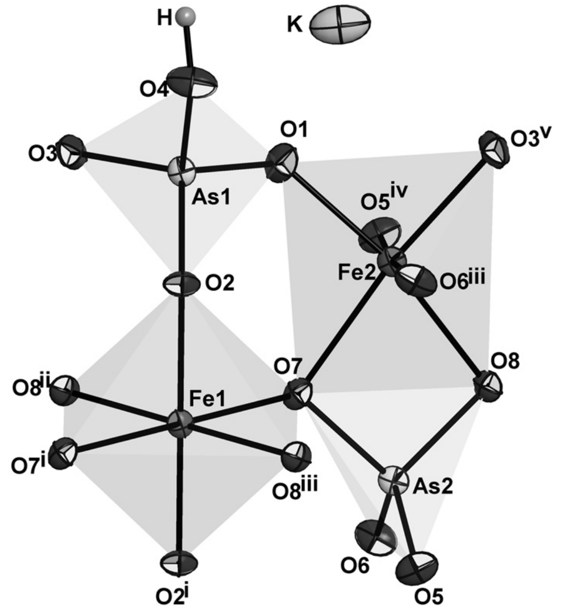

Fig. 4. Ellipsoid drawing (70 % probability) of $KFe_3(AsO_4)_2(HAsO_4)_2$ (^{i} 0.5 – *x*, 1.5 – *y*, 1 – *z*; ^{ii} *x*, 1 – *y*, 0.5 + *z*; ^{iii} 0.5 – *x*, 0.5 + *y*, 0.5 – *z*; ^{iv} 0.5 – *x*, –0.5 + *y*, 0.5 – *z*; ^{v} *x*, 1 – *y*, –0.5 + *z*).

1.730(2) Å, see Table 4). This leads to a rather large mean As-O bond length of the $As2O_4$ tetrahedra of 1.694 Å, *versus* 1.683 Å for $As1O_4$ and 1.682 Å for literature data on arsenates (Baur, 1981). The BVS for As2 is therefore slightly decreased (4.90 v.u.). The angles O7-As2-O8 (93.09(11)°) and O8-Fe2-O7 (73.57(9)°) are extremely narrow due to the Fe-As repulsion across the shared O7-O8 edge. The remaining angles in both $As2O_4$ and $Fe2O_6$ all become wider, thus compensating the two narrow angles and leading to normal average O-As2-O and O-Fe2-O angles. However, the bond-angle distortions of $As2O_4$ and $Fe2O_6$ are both very large (σ^2 = 66.3 for $As2O_4$ *versus* 10.5 for $As1O_4$; σ^2 = 45.2 for $Fe2O_6$ *versus* 16.5 for $Fe1O_6$; Table 3a).

The shared O-O edge also influences the Fe-O distances in the involved FeO_6 octahedra. The largest distances in both FeO_6 polyhedra are therefore to the two O atoms sharing edges with the AsO_4 tetrahedra, but the influence on the FeO_6 polyhedra compared to the involved AsO_4 tetrahedra is much less perceptible.

$KFe_3(AsO_4)_2(HAsO_4)_2$-type – Comparison to related structure types

Shared edges between tetrahedra and octahedra are fairly rare; however, there are a number of phosphates and arsenates that show this uncommon feature. The four most closely related types in terms of element composition are further described below, three of those are also structurally closely related to the novel $KFe_3(AsO_4)_2(HAsO_4)_2$. The shared edge between PO_4 and FeO_6 in $K_3Fe_2(PO_4)_3$ (*C*2/*c*) (Pintard-Screpel & d'Yvoire, 1983) leads to the formation of a framework structure, which is totally different to what is encountered in the novel compound. On the other hand $K_3Fe_3(PO_4)_4{\cdot}H_2O$ (*Pnna*) (Lii, 1995), $K_3Fe_3(AsO_4)_4$ (Ouerfelli *et al.*, 2005) and isotypic $K_3Cr_3(AsO_4)_4$ (*Cmca*) (Friaa *et al.*, 2003) show strong relations to the new structural type (Figs. 5 and 6). The main feature in these three compounds are the $(Fe/Cr)_2(As/P)_2O_{15}$-groups which are connected to identical layers. The main differences arise in the connectivities of the layers, the space group and symmetry. The novel compound shows the closest distance between adjacent layers, which is a result of the hydrogen bonds connecting them, compared to the other three compounds in which the layers are also shifted (compare Fig. 6a–d). The novel type contains only one K atom per formula unit (charge balance being achieved through H atoms), while all other types contain three K atoms. The positions of the K atoms are the only slight difference between the Fe and Cr members of the isostructural $K_3M_3^{3+}(AsO_4)_4$ type.

In $K_3Fe_3(PO_4)_4{\cdot}H_2O$ the connection between adjacent layers is achieved through hydrogen bonds of water molecules, but the topology is otherwise nearly identical to that of the novel type. This close relationship is easily seen in Fig. 6a–d. The s-curved layers are parallel to each other in the two isotypic $K_3M_3^{3+}(AsO_4)_4$ compounds; in $K_3Fe_3(PO_4)_4{\cdot}H_2O$ and $KFe_3(AsO_4)_2(HAsO_4)_2$, however, two adjacent layers are shifted by 1/2 and the AsO_4 tetrahedra point towards each other. The acceptor oxygen atoms of the water molecule in the phosphate become the donor atoms of the hydrogen bonds in the new compound.

Of course also the stoichiometry of these three related structure types differs; this can for some part be explained by the different synthesis conditions. $K_3M_3^{3+}(AsO_4)_4$(M^{3+} = Fe, Cr) were both synthesized by high-temperature solid state reactions ($T_{\max}$ = 1173 K) (Friaa *et al.*, 2003; Ouerfelli *et al.*, 2005); $K_3Fe_3(PO_4)_4{\cdot}H_2O$ (Lii, 1995) was also synthesized under relatively high temperatures (823 K), but under hydrothermal high-pressure conditions. The new compound, on the other hand, was synthesized hydrothermally at much lower temperature (493 K). Incorporation of H or H_2O would not have been possible through solid state reactions. In the new compound two H atoms appear in the structure to provide charge balance for the two missing K atoms, which are present in all three other compounds. It is not clear why the new structure type contains 2/3 less K than the other three types, because the results of the synthesis (95 vol.-% $K(H_2O)Fe(H_{1.5}AsO_4)_2(H_2AsO_4)$ and 5 vol.-% $KFe_3(AsO_4)_2(HAsO_4)_2$) prove that sufficient K was available in the reaction to allow the formation of the $M_3^{1+}M_3^{3+}(AsO_4)_4$-type.

The protonation of the new compound was caused by the highly acidic synthesis conditions and provides additional bond-strength between the layers.

Description of the crystal structures of $K(H_2O)M^{3+}(H_{1.5}AsO_4)_2(H_2AsO_4)$($M^{3+}$ = Fe, Ga, In)

The isotypic compounds II, III, and IV are monoclinic (*P*2/*n*) and have 15 atoms in the asymmetric unit. The

Table 3a. Selected bond-distances [Å], bond angles [°] and distortion parameters* for $KFe_3(AsO_4)_2(HAsO_4)_2$.

K1-O1	2.732(3) 2×	Fe2-O8	2.084(2)	O1-Fe2-O5	86.34(10)
K1-O5	2.786(2) 2×	Fe2-O7	2.105(3)	O3-Fe2-O5	89.21(11)
K1-O4	2.796(3) 2×	⟨Fe1-O⟩	2.016	O1-Fe2-O6	95.12(10)
K1-O3	3.157(3) 2×	BVS	3.03	O3-Fe2-O6	85.81(10)
⟨K1-O⟩	2.868	Δ	0.00090	O3-Fe2-O8	100.23(10)
BVS[1]	1.13			O5-Fe2-O8	88.62(10)
		O1-As1-O2	111.18(12)	O6-Fe2-O8	90.87(10)
As1-O1	1.667(2)	O1-As1-O3	110.52(13)	O1-Fe2-O7	96.03(10)
As1-O2	1.670(2)	O2-As1-O3	111.63(12)	O5-Fe2-O7	95.06(10)
As1-O3	1.672(2)	O1-As1-O4	111.02(14)	O6-Fe2-O7	89.74(9)
As1-O4	1.721(2)	O2-As1-O4	103.04(12)	O8-Fe2-O7	73.57(9)
⟨As1-O⟩	1.683	O3-As1-O4	109.23(13)	⟨O-Fe2-O⟩	90.10
BVS[2]	5.04	⟨O-As1-O⟩	109.44	σ^2	45.2
Δ	0.000176	σ^2	10.5		
				Hydrogen bonds	
As2-O5	1.656(2)	O5-As2-O6	109.91(12)	O4-H	0.88(2)
As2-O6	1.664(2)	O5-As2-O7	114.50(12)	H···O6	2.15(4)
As2-O7	1.725(2)	O6-As2-O7	113.42(12)	O4-H···O6	2.921(3)
As2-O8	1.730(2)	O5-As2-O8	111.29(12)	< O4-H-O6	146(6)
⟨As1-O⟩	1.694	O6-As2-O8	113.82(12)		
BVS[2]	4.90	O7-As2-O8	93.09(11)	O4-H	0.88(2)
Δ	0.000401	⟨O-As2-O⟩	109.34	H··· O3	2.20(5)
		σ^2	66.3	O4-H···O3	2.865(4)
Fe1-O2	1.942(2) 2×			< O4-H-O3	132(6)
Fe1-O8	2.032(2) 2×	O2-Fe1-O8	92.55(10) 2×		
Fe1-O7	2.083(2) 2×	O2-Fe1-O8	87.45(10) 2×	BVS O1	2.12
⟨Fe1-O⟩	2.019	O2-Fe1-O7	86.50(10) 2×	BVS O2	1.91
BVS[2]	3.01	O2-Fe1-O7	93.50(10) 2×	BVS O3	1.92
Δ	0.00083	O8-Fe1-O7	84.85(10) 2×	BVS O4(OH)	1.29
		O8-Fe1-O7	95.15(10) 2×	BVS O5	2.03
Fe2-O1	1.934(3)	⟨O-Fe1-O⟩	90.00	BVS O6	1.83
Fe2-O3	1.968(3)	σ^2	16.5	BVS O7	1.93
Fe2-O5	1.999(2)			BVS O8	2.00
Fe2-O6	2.008(2)	O1-Fe2-O3	90.59(11)		

[1] (Wood & Palenik, 1999), [2] (Brown & Aldermatt, 1985). * Bond-length distortion (Brown & Shannon, 1973): $\Delta = \frac{1}{6}\sum_{i=1}^{6}[(R_i - \overline{R})/\overline{R}]^2$ for octahedra, $\frac{1}{4}\sum_{i=1}^{4}[(R_i - \overline{R})/\overline{R}]^2$ for tetrahedra; bond-angle distortion (Robinson *et al.*, 1971): $\sigma^2 = \sum_{i=1}^{12}(\theta_i - 90°)^2/11$ for octahedra, $\sum_{i=1}^{6}(\theta_i - 109.47°)^2/5$ for tetrahedra.

M^{3+} cations, As2 and O7 (water molecule) lie on the two-fold axis, while all other atoms occupy general positions. Two atoms occupy split positions slightly off the respective centres of symmetry linking the two split sites, these are the K atom (K-K ~ 1–1.5 Å) and H4 which is involved in a very short hydrogen bond (2.499(10)–2.516(9) Å, see Table 5).

The crystal structure is built of $M^{3+}O_6$ octahedra which corner-link to six AsO_4 tetrahedra to form decorated kröhnkite-like chains (Kolitsch & Fleck, 2006) extending parallel to [100] (Fig. 7). The 7-coordinated K atoms (⟨K-O⟩ = 2.803–2.845 Å) lie in-between these chains, as does one water molecule (O7). The two non-equivalent AsO_4 polyhedra are both protonated and the resulting medium to very strong hydrogen bonds (Table 5) are the main force connecting the chains in the structure leading to a rather complex connectivity.

The hydrogen bonding scheme of $As1O_4$ involves the very strong split double well position (H4) and a second medium strong hydrogen bond (H2); $As1O_4$ is therefore 1.5 times protonated. Furthermore, the polyhedron is also the acceptor of 2.5 hydrogen bonds (Table 5). $As2O_4$ is doubly protonated with two symmetry-related medium strong hydrogen bonds (2.662(4)–2.685(7) Å), which are accepted by the O7 atom of the water molecule. The H_2O unit is thus strongly held in place by these bonds and its own two hydrogen atoms, which are accepted by the $As1O_4$ polyhedra of an adjacent kröhnkite-type chain. This demonstrates that the chains are very firmly connected to each other by numerous hydrogen bonds in various directions (Fig. 8a).

The As-OH bonds are considerably elongated compared to the As-O bonds, which is typical for protonated AsO_4 tetrahedra (Ferraris & Ivaldi, 1984) and leads to strongly distorted polyhedra. The mean As-O bond lengths in all AsO_4 tetrahedra of the three isotypic compounds range from 1.686–1.697 Å, which is considerably longer than the average bond length for AsO_4 tetrahedra of 1.682 Å

Table 3b. Selected bond-distances [Å], bond angles [°] and distortion parameters* for $K(H_2O)M^{3+}(H_{1.5}AsO_4)_2(H_2AsO_4)$ (M^{3+} = Fe, Ga, In).

$K(H_2O)Fe(H_{1.5}AsO_4)_2(H_2AsO_4)$		**$K(H_2O)Ga(H_{1.5}AsO_4)_2(H_2AsO_4)$**		**$K(H_2O)ln(H_{1.5}AsO_4)_2(H_2AsO_4)$**	
K-O2	2.691(4)	K-O6	2.674(4)	K-O4	2.751(7)
K-O6	2.710(5)	K-O2	2.686(3)	K-O2	2.758(6)
K-O4	2.782(5)	K-O4	2.762(4)	K-O6	2.760(7)
K-O2	2.809(4)	K-O2	2.816(3)	K-O2	2.803(6)
K-O6	2.873(5)	K-O6	2.836(4)	K-O4	2.882(7)
K-O4	2.950(5)	K-O5	2.922(3)	K-O5	2.918(6)
K-O5	2.954(4)	K-O4	2.923(4)	K-O6	3.041(8)
<K-O>	**2.824**	**<K-O>**	**2.803**	**<K-O>**	**2.845**
BVS^1	**1.06**	**BVS**	**1.12**	**BVS**	**1.00**
Fe-O2	1.993(3) 2x	Ga-O2	1.952(2) 2x	ln-O2	2.123(4) 2x
Fe-O5	2.019(3) 2x	Ga-O5	1.978(2) 2x	ln-O5	2.139(5) 2x
Fe-O1	2.026(3) 2x	Ga-O1	1.988(2) 2x	ln-O1	2.139(5) 2x
<Fe-O>	**2.013**	**<Ga-O>**	**1.973**	**<ln-O>**	**2.134**
BVS^2	**3.03**	**BVS**^{2}	**3.12**	**BVS**^{2}	**3.21**
Δ	**4.98×10^{-5}**	Δ	**5.92×10^{-5}**	Δ	**1.25×10^{-5}**
As1-O1	1.671(3)	As1-O1	1.671(2)	As1-O1	1.668(4)
As1-O2	1.672(3)	As1-O2	1.671(2)	As1-O2	1.670(4)
As1-O3	1.686(3)	As1-O3	1.685(3)	As1-O3	1.697(5)
As1-O4	1.718(3)	As1-O4	1.725(3)	As1-O4	1.726(5)
<As1-O>	**1.687**	**<As1-O>**	**1.688**	**<As1-O>**	**1.690**
BVS^2	**4.98**	**BVS**^{2}	**4.96**	**BVS**^{2}	**4.93**
Δ	**0.00013**	Δ	**0.0017**	Δ	**0.00020**
As2-O5	1.662(3) 2x	As2-O5	1.662(2) 2x	As2-O5	1.665(5) 2x
As2-O6	1.718(3) 2x	As2-O6	1.716(3) 2x	As2-O6	1.728(5) 2x
<As2-O>	**1.690**	**<As2-O>**	**1.689**	**<As2-O>**	**1.697**
BVS^2	**4.94**	**BVS**	**4.95**	**BVS**	**4.86**
Δ	**0.00027**	Δ	**0.0026**	Δ	**0.00034**
O2-Fe-O5	90.93(12) 2x	O2-Ga-O5	89.44(10) 2x	O2-ln-O5	90.11(19) 2x
O2-Fe-O5	89.78(13) 2x	O2-Ga-O5	89.84(10) 2x	O2-ln-O5	92.33(18) 2x
O5-Fe-O5	88.08(18)	O5-Ga-O5	88.45(15)	O5-ln-O5	86.6(3)
O2-Fe-O1	87.72(13) 2x	O2-Ga-O1	88.69(10) 2x	O2-ln-O1	91.4(2) 2x
O2-Fe-O1	91.60(13) 2x	O2-Ga-O1	92.02(10) 2x	O2-ln-O1	86.2(2) 2x
O5-Fe-O1	89.94(12) 2x	O5-Ga-O1	90.27(10) 2x	O5-ln-O1	90.39(19) 2x
O1-Fe-O1	92.15(17)	O1-Ga-O1	91.05(14)	O1-ln-O1	92.8(2)
<O-Fe-O>	**90.01**	**<O-Ga-O>**	**90.00**	**<O-ln-O>**	**90.02**
σ^2	**2.33**	σ^2	**1.45**	σ^2	**5.76**
O1-As1-O2	117.22(15)	O1-As1-O2	117.76(11)	O1-As1-O2	117.1(3)
O1-As1-O3	106.99(15)	O1-As1-O3	106.65(13)	O1-As1-O3	106.3(2)
O2-As1-O3	112.04(16)	O2-As1-O3	112.51(13)	O2-As1-O3	112.3(2)
O1-As1-O4	111.50(16)	O1-As1-O4	111.69(13)	O1-As1-O4	111.3(3)
O2-As1-O4	100.95(16)	O2-As1-O4	100.71(13)	O2-As1-O4	100.4(2)
O3-As1-O4	107.80(17)	O3-As1-O4	107.09(14)	O3-As1-O4	109.2(3)
<O-As1-O>	**109.42**	**<O-As1-O>**	**109.40**	**<O-As1-O>**	**109.43**
σ^2	**30.46**	σ^2	**34.65**	σ^2	**32.39**
O5-As2-O5	120.9(2)	O5-As2-O5	121.49(17)	O5-As2-O5	120.1(4)
O5-As2-O6	111.20(16) 2x	O5-As2-O6	111.74(13) 2x	O5-As2-O6	103.0(2) 2x
O5-As2-O6	103.13(15) 2x	O5-As2-O6	102.60(12) 2x	O5-As2-O6	110.9(3) 2x
O6-As2-O6	106.7(3)	O6-As2-O6	105.9(2)	O6-As2-O6	108.7(4)
<O-As2-O>	**109.4**	**<O-As2-O>**	**109.35**	**<O-As2-O>**	**109.43**
σ^2	**44.94**	σ^2	**52.38**	σ^2	**40.28**

BVSs for O-atoms: O1 = 1.78/1.79/1.83; O2 = 2.19/2.21/2.18; O3(OH) = 1.24/1.25/1.21; O4(OH) = 1.41/1.41/1.42; O5 = 1.93/1.95/1.96, O6(OH) = 1.47/1.51/1.37 for compounds II, III and IV, respectively. [1] (Wood & Palenik, 1999); [2] (Brown & Aldermatt, 1985). * Bond-length distortion (Brown & Shannon, 1973): $\Delta = \frac{1}{6}\sum_{i=1}^{6}[(R_i-\overline{R})/\overline{R}]^2$ for octahedra, $\frac{1}{4}\sum_{i=1}^{4}[(R_i-\overline{R})/\overline{R}]^2$ for tetrahedra; bond-angle distortion (Robinson *et al.*, 1971): $\sigma^2 = \sum_{i=1}^{12}(\theta_i-90°)^2/11$ for octahedra, $\sum_{i=1}^{6}(\theta_i-109.47°)^2/5$ for tetrahedra.

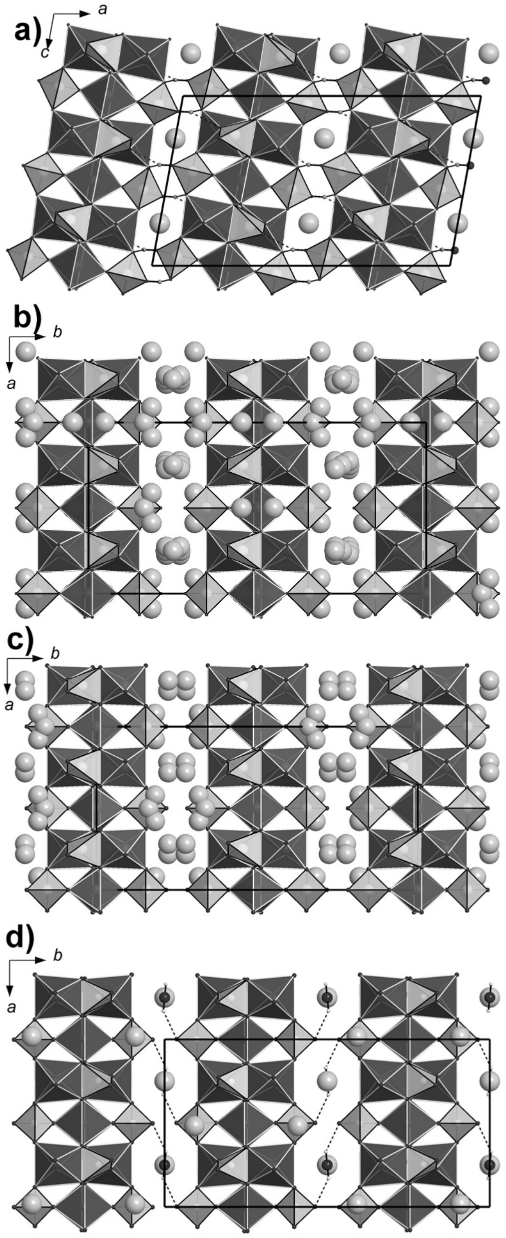

Fig. 5. The crystal structure of $KFe_3(AsO_4)_2(HAsO_4)_2$ (**a**) parallel [010] compared to $K_3Fe_3(AsO_4)_4$ (**b**), $K_3Cr_3(AsO_4)_4$ (**c**) and $K_3Fe_3(PO_4)_4{\cdot}H_2O$ (**d**) parallel to the corresponding direction [001].

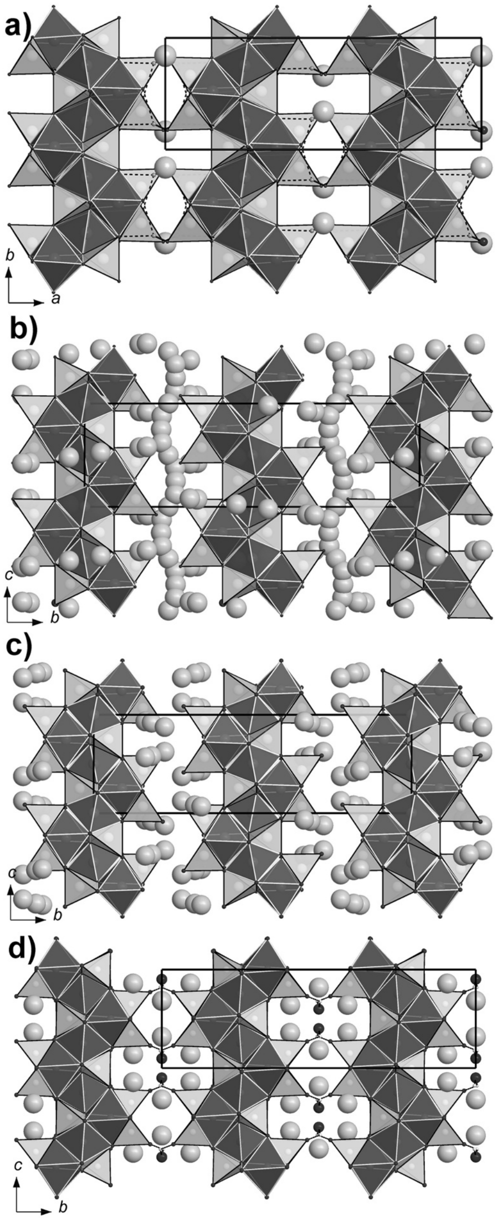

Fig. 6. The crystal structure of $KFe_3(AsO_4)_2(HAsO_4)_2$ (**a**) parallel [001] compared to $K_3Fe_3(AsO_4)_4$ (**b**), $K_3Cr_3(AsO_4)_4$ (**c**) and $K_3Fe_3(PO_4)_4{\cdot}H_2O$ (**d**) parallel to the corresponding direction [100].

(Baur, 1981) and a result of the protonation. Interestingly, the $As2O_4$ polyhedra are more distorted than the $As1O_4$ polyhedra, although $As2O_4$ shows point symmetry 2 *versus* 1 for $As1O_4$ (Table 3b), but of course $As2O_4$ is doubly protonated.

The unit-cell axes and volumes of these three isotypic compounds rise with rising ionic radius of the M^{3+} atoms, as expected. The same is also true for all mean bond lengths and bond angles in the structures, excluding As and the H atoms and their bonds. The shortest hydrogen bond is encountered in the In compound with only 1.499(10) Å. The calculated BVSs (calculated without the contribution of H-bonds) show quite good agreement with the expected values (see Table 3b). All but two O atoms (O2 and O5) are involved in hydrogen bonds and therefore have BVSs significantly smaller than 2.

$K(H_2O)M^{3+}(H_{1.5}AsO_4)_2(H_2AsO_4)$-type – Comparison to related structure types

The novel structure type shows very close relationships to two other structure types, namely $CsGa(H_{1.5}AsO_4)_2(H_2AsO_4)$ and isotypic $CsCr(H_{1.5}AsO_4)_2(H_2AsO_4)$ (Schwendtner & Kolitsch, 2005b) crystallizing in space group $C2/c$ and topologically identical $CsAl(H_{1.5}AsO_4)_2(H_2AsO_4)$ (Schwendtner & Kolitsch,

Table 4. Selected distances of atoms involved in edge-sharing between AsO_4 tetrahedra and $M^{3+}O_6$ octahedra (M^{3+} = Fe, Cr).

Compound	As-O(edge)	O-O(edge)	As-Fe(edge)
$KFe_3(AsO_4)_2(HAsO_4)_2$	1.725(2) 1.730(2)	2.509	2.8656(8)
$K_3Fe_3(AsO_4)_4$[1]	1.729(5) 2×	2.516(8)	2.881
$K_3Cr_3(AsO_4)_4$[2]	1.739(4) 2×	2.488(8)	2.826

[1] (Ouerfelli *et al.*, 2005); [2] (Friaa *et al.*, 2003).

Table 5. Hydrogen bonds in $K(H_2O)M^{3+}(H_{1.5}AsO_4)_2(H_2AsO_4)$ with M^{3+} = Fe, Ga, In (in lines 1, 2 and 3, respectively).

D-H···A	*d*(D-H) [Å]	*d*(H-A) [Å]	*d*(D···A) [Å]	< DHA [°]
O6-H1···O7	0.89(2)	1.82(3)	2.671(4)	160(6)
O6-H1···O7	0.89(2)	1.79(2)	2.662(4)	167(7)
O6-H1···O7	0.89(2)	2.00(9)	2.685(7)	133(11)
O4-H2···O3	0.89(2)	1.87(2)	2.741(5)	167(6)
O4-H2···O3	0.89(2)	1.86(2)	2.739(4)	170(6)
O4-H2···O3	0.90(2)	2.05(8)	2.733(7)	131(9)
O7-H3···O1	0.913(3)	1.944(3)	2.759(5)	147.7(2)
O7-H3···O1	0.867(19)	1.96(3)	2.764(4)	153(4)
O7-H3···O1	0.91(2)	2.00(6)	2.765(7)	142(8)
O3-H4···O3	0.843(3)	1.692(3)	2.516(6)	165.07(12)
O3-H4···O3	0.89(2)	1.63(3)	2.506(5)	168(9)
O3-H4···O3	0.90(2)	1.62(5)	2.499(10)	166(20)

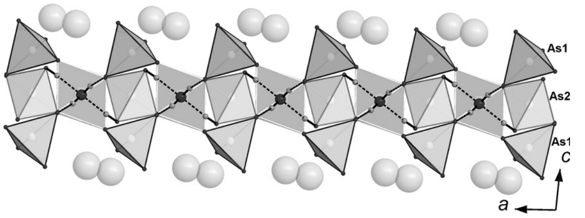

Fig. 7. The decorated kröhnkite-type (octahedral-tetrahedral) chain in compounds II, III and IV.

2007a) crystallizing in *Cc* (compare Fig. 8a–c). The latter three structures share topologically identical kröhnkite-type (octahedral-tetrahedral) chains (Kolitsch & Fleck, 2006) but the connection between the chains, which is practically identical in the three Cs-compounds, is slightly different in the novel type, as becomes apparent from the respective chemical formula: unlike $K(H_2O)M^{3+}(H_{1.5}AsO_4)_2(H_2AsO_4)$, none of the three Cs-compounds contains any water. This is very probably due to the small K^+ cation (compared to Cs^+) occupying the voids between the chains. The Cs-sites are well-defined and 10-coordinated in both *C*2/*c* and *Cc* types. In order to fit the smaller K atom into the same void, the chains have to shift considerably closer together. From the strong dislocation that actually leads to a split position of the K atom slightly off the centre of symmetry it becomes apparent that this shift is not sufficient to provide a perfect fit for the K-atom. Furthermore, in direction parallel to *b* the chains move apart to allow the incorporation of H_2O molecules. This in turn makes it possible that adjacent chains parallel *c* move closer together, thus making the void incorporating the M^{1+} atoms smaller.

These shifts in the unit cell are also reflected by the unit-cell parameters of these closely related compounds. In direction *a* (which is the elongation direction of the kröhnkite-type chains) the unit-cell parameters are very similar (4.641(1)–4.798(10) Å for the K-compounds and 4.634(1)–4.744(1) Å for the Cs-compounds), because they are unaffected by the M^{1+} ions and chain shifts. The unit-cell parameter *b*, however, is strongly elongated (17.392–17.664 Å, for the, due to different cell settings, doubled *b* length of the K-compounds, compared to 14.625(3)–14.674(3) Å for the three Cs-compounds). This must be expected due to the insertion of two H_2O in that direction. Exactly the opposite happens in direction *c*, which is the one most strongly influenced by the M^{1+} cations. In the three new K-compounds the unit-cell parameters *c* are therefore considerably shorter (13.772(3)–13.971(3) Å) than the equivalent parameters in the three Cs-compounds (15.127(3)–15.162(3) Å). The volumes of the unit cells are more influenced by the additional water than the differences in cation size. They are therefore considerably larger for the doubled unit cells of the three new H_2O-containing K-compounds (1107.8–1180.2 Å^3, compared to 1028.7(4)–1047.6(4) Å^3 for the three Cs-compounds).

Raman spectroscopy

The Raman spectra of the two of $K(H_2O)M^{3+}(H_2AsO_4)(H_{1.5}AsO_4)_2$($M^{3+}$ = Fe, Ga) modifications are very complex (Fig. 9), due to the different protonated AsO_4 polyhedra and their low symmetry. The spectral range between 950 and 700 cm^{-1} shows the As-O stretching modes of the protonated AsO_4 groups, where the strong bands centered at 849 and 867 cm^{-1} in the Fe-compound (rather weak in the Ga-compound) can be attributed to the symmetric stretching vibrations of the two AsO_4 groups. The very intense bands centred at 759/775 and 763/776 cm^{-1} for the Fe and Ga-compounds respectively represent the antisymmetric stretching vibrations of the AsO_4 polyhedra. Due to the distortion of the polyhedra splitting and additional bands can be expected, different intensities of the bands are likely because of the measurement of arbitrarily oriented single crystals. The bands in the spectral region below 500 cm^{-1} are assigned to various bending vibrations of the AsO_4 polyhedra, vibrations of the $M^{3+}O_6$ octahedra and lattice modes. No bands could be observed in the region between 1000 and 4000 cm^{-1}, the area between 2000 and 4000 cm^{-1} showed strong effects of luminescence.

Possible occurrences in nature

The two new K-Fe^{3+}-arsenates have crystallized at mild hydrothermal conditions at very low pH ($\leqslant 1$). Although such

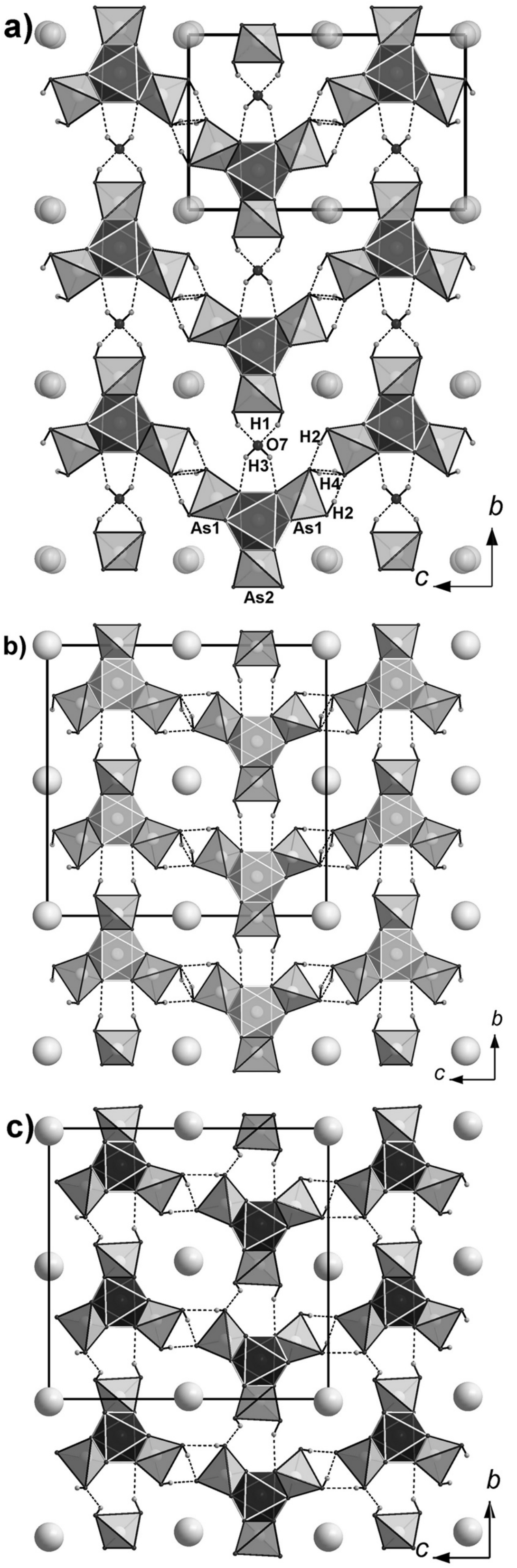

Fig. 8. The connectivity in the crystal structure of $K(H_2O)Fe(H_2AsO_4)(H_{1.5}AsO_4)_2$ (**a**) compared to that in related $CsGa(H_2AsO_4)(H_{1.5}AsO_4)_2$ (**b**) and related $CsAl(H_2AsO_4)(H_{1.5}AsO_4)_2$ (**c**), viewed along [100].

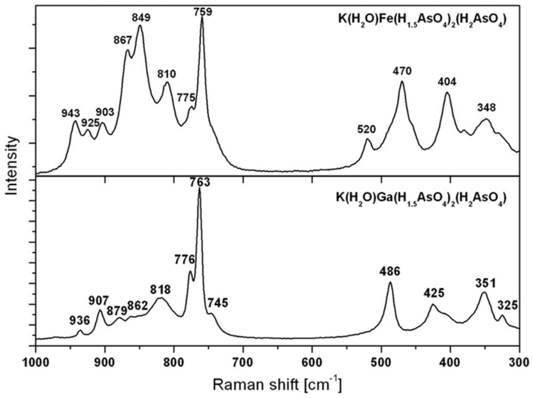

Fig. 9. Single-crystal Raman spectra of $K(H_2O)M^{3+}(H_2AsO_4)(H_{1.5}AsO_4)_2(M^{3+} = Fe, Ga)$.

strongly acidic conditions would be rare in natural environments, they may be encountered in underground mines or locally in mining dumps. Thus, these two arsenates may also exist as minerals in nature. The recent discovery of the two highly acidic K-Fe^{3+}-phosphate minerals gengenbachite and haigerachite (see Introduction) indicates that acidic K-Fe^{3+}-arsenates could also be stable in specific natural environments.

It seems desirable to investigate the system K-Fe^{3+}-As-O-H in more detail at different temperatures and in different pH regimes, and to assess the stability of the observed crystalline phases.

Acknowledgements: Financial support by a DOC-FFORTE (Frauen in Forschung und Technologie) Fellowship of the Austrian Academy of Sciences (ÖAW) to K. Schwendtner is gratefully acknowledged.
Two anonymous referees are thanked for helpful comments.

References

Anisimova, N., Chudinova, N., Serafin, M. (1997): Preparation and crystal structure of potassium iron hydrogen phosphate $KFe_3(HPO_4)_2(H_2PO_4)_6.4(H_2O)$, *Z. Anorg. Allg. Chem.*, **623**, 1708-1714.

Baran, E.J., Schwendtner, K., Kolitsch, U. (2006a): Vibrational spectra of $ScAsO_4{\cdot}H_2O$, *J. Raman Spectrosc.*, **37**, 1453-1455.

Baran, E.J., Schwendtner, K., Kolitsch, U. (2006b): Vibrational spectra of three new diarsenates containing scandium (III). *J. Raman Spectrosc.*, **37**, 1335-1340.

Baur, W.H. (1981): Interatomic distance predictions for computer simulation of crystal structures. Academic Press, New York, 31-52.

Birch, W.D., Pring, A., Self, P.G., Gibbs, R.B., Keck, E., Jensen, M.C., Foord, E.E. (1996): Meurigite, a new fibrous iron phosphate resembling kidwellite. *Mineral. Mag.*, **60**, 787-793.

Brown, I.D. & Aldermatt, D. (1985): Bond-valence parameters obtained from a systematic analysis of the inorganic crystal structure database. *Acta Crystallogr.*, **B41**, 244-247.

Brown, I.D. & Shannon, R.D. (1973): Empirical bond-strength-bond-length curves for oxides. *Acta Crystallogr.*, **A29**, 266-282.

Chang, R.S., Wang, S.L., Lii, K.H. (1997): Layered iron(III) arsenates: synthesis and characterization of $A_2Fe_2O(AsO_4)_2$ (A = K, Rb). *Inorg. Chem.*, **36**, 3410-3413.

Ferraris, G. & Ivaldi, G. (1984): X-OH and O-H· · ·O bond lengths in protonated oxyanions. *Acta Crystallogr.*, **B40**, 1-6.

Friaa, B.B., Boughzala, H., Jouini, T. (2003): Tripotassium trichromium(III) tetraarsenate $K_3Cr_3(AsO_4)_4$: synthesis, structural study, IR spectroscopy characterization and ionic behavior. *J. Solid State Chem.*, **173**, 273-279.

Kolitsch, U. (1999): Evidence for the identity of meurigite and phosphofibrite by transmission electron microscopy and X-ray powder diffraction. *Eur. J. Mineral.*, **11** Beih. 1, 132.

Kolitsch, U. (2004): Crystal structure of ammonium scandium diarsenate(V), $(NH_4)ScAs_2O_7$, the second $KAlP_2O_7$-type diarsenate. *Z. Krist. - New Cryst. Struct.*, **219**, 207-208.

Kolitsch, U. & Fleck, M. (2006): Third update on compounds with kröhnkite-type chains: the crystal structure of wendwilsonite $[Ca_2Mg(AsO_4)_2{\cdot}2H_2O]$ and the new triclinic structure types of $AgSc(CrO_4)_2{\cdot}2H_2O$ and $M_2Cu(Cr_2O_7)_2{\cdot}2H_2O$ (M = Rb, Cs). *Eur. J. Mineral.*, **18**, 471-482.

Kolitsch, U. & Schwendtner, K. (2004): Crystal structure of scandium arsenate(V) monohydrate, $ScAsO_4{\cdot}H_2O$, the first $MnMoO_4{\cdot}H_2O$-type arsenate. *Z. Krist. - New Cryst. Struct.*, **219**, 347-348.

Kolitsch, U. & Schwendtner, K. (2005): The octahedral-tetrahedral framework structures of $InAsO_4{\cdot}H_2O$ and $PbIn(AsO_4)(AsO_3OH)$. *Acta Crystallogr.,* **C61**, i86-i98.

Lii, K.H. (1995): $K_3Fe_3(PO_4)_4{\cdot}H_2O$: an iron(III) phosphate with a layer structure. *Eur. J. Sol. State Inorg. Chem.*, **32**, 917-926.

Moore, P.B. (1972): Octahedral tetramer in the crystal structure of leucophosphite, $K_2[Fe^{3+4}(OH)_2(H_2O)_2(PO_4)_4]{\cdot}2H_2O$. *Am. Mineral.*, **57**, 397-410.

Otwinowski, Z., Borek, D., Majewski, W., Minor, W. (2003): Multiparameter scaling of diffraction intensities. *Acta Crystallogr.*, **A59**, 228-234.

Otwinowski, Z. & Minor, W. (1997): Processing of X-ray diffraction data collection in oscillation mode. *Methods Enzymol.*, **276**, 307-326.

Ouerfelli, N., Zida, M.F., Jouini, T. (2005): Composé à charpente bidimensionnelle $K_3Fe_3(AsO_4)_4$. *Acta Crystallogr.*, **E61**, i67-i69.

Pintard-Screpel, M. & d'Yvoire, F. (1983): Structure de l'orthophosphate de difer(III) et de tripotassium, $K_3Fe_2(PO_4)_3$. *Acta Crystallogr.*, **C39**, 9-12.

Robinson, K., Gibbs, G.V., Ribbe, P.H. (1971): Quadratic elongation: A quantitative measure of distortion in coordination polyhedra. *Science*, **172**, 567-570.

Schwendtner, K. (2006): $TlInAs_2O_7$, $RbInAs_2O_7$, and $(NH_4)InAs_2O_7$: synthesis and crystal structure of three isotypic diarsenates - representatives of a novel microporous structure type. *J. Alloy. Compd.*, **421**, 57-63.

Schwendtner, K. & Kolitsch, U. (2004a): Alkali scandium arsenates. I. The framework structures of $KSc(HAsO_4)_2$ and $RbScAs_2O_7$. *Acta Crystallogr.,* **C60**, i79-i83.

Schwendtner, K. & Kolitsch, U. (2004b): Alkali scandium arsenates. II. The framework structures of α- and β-$CsSc(HAsO_4)_2$. *Acta Crystallogr.,* **C60**, i84-i88.

Schwendtner, K. & Kolitsch, U. (2005a): Compounds in the system $M^{1+}M^{3+}As_2O_7$(M^{1+} = Li, Na, K, Rb, Cs, Ag, Tl, NH_4; M^{3+} = Al, Ga, In, Sc, Cr, Fe): novel representatives and an overview. *Mitt. Österr. Mineral. Ges.,* **151**, 109.

Schwendtner, K. & Kolitsch, U.(2005b):$CsGa(H_{1.5}AsO_4)_2(H_2AsO_4)$ and isotypic $CsCr(H_{1.5}AsO_4)_2(H_2AsO_4)$: decorated kröhnkite-like chains in two unusual hydrogen arsenates. *Acta Crystallogr. ,* **C61**, i90-i93.

Schwendtner, K. & Kolitsch, U. (2005c): Novel compounds in the system $M^{1+}M^{3+}(HAsO_4)_2$(M^{1+} = Li, Na, K, Rb, Cs, Ag, Tl; M^{3+} = Al, Ga, In, Sc, Cr, Fe) - an overview. *Mitt. Österr. Mineral. Ges.,* **151**, 110.

Schwendtner, K. & Kolitsch, U. (2007a): $CsAl(H_2AsO_4)_2(HAsO_4)$ - a new monoclinic protonated arsenate with decorated kröhnkite-like chains. *Acta Crystallogr.,* **C63**, i17-i20.

Schwendtner, K. & Kolitsch, U. (2007b): Octahedrally coordinated As in M^{1+}-arsenates – architecture and seven new members. *Acta Crystallogr.*, **B63**, 205-215.

Schwendtner, K., Kolitsch, U., Tillmanns, E. (2006a): $Al(H_2AsO_4)(H_2As_2O_7)$ - a novel strongly acidic structure type and the first structural characterization of a diprotonated diarsenate group. 19*th* General Meeting of the International Mineralogical Association, Kobe, Japan, p. 90387.

Schwendtner, K., Kolitsch, U., Tillmanns, E. (2006b): $K(H_3O)M^{3+}(HAsO_4)_2(H_2AsO_4)$($M^{3+}$ = In, Ga, Fe) - three members of a novel structure type. *Z. Krist. Suppl.,* **24**, 119.

Schwendtner, K., Kolitsch, U., Tillmanns, E. (2006c): ${M^{1+}}_3{M^{3+}}_2(HAs_2O_7)_3{\cdot}x(H_3AsO_4)$($M^{1+}$, M^{3+} = NH_4, Al / Rb, Al / Tl, Ga; x = 0.75 / 1) - a novel structure type with large channels hosting M^{1+}-cations and arsenic acid. 15*th* Slovenian - Croatian Crystallographic Meeting, Jezersko, Slovenia, p. 36.

Sheldrick, G.M. (1997a): SHELXL-97, a program for crystal structure refinement. University of Göttingen, Göttingen, Germany.

Sheldrick, G.M. (1997b): SHELXS-97, a program for the solution of crystal structures. University of Göttingen, Göttingen, Germany.

Takano, M., Takada, T., Wada, T., Okada, K. (1971): Magnetic properties of scorodite ($FeAsO_4{\cdot}2H_2O$) and pharmacosiderite ($KFe_4(AsO_4)_3{\cdot}8H_2O$). *J. Phys. Soc. Jpn.,* **31**, 298.

Waerstad, K.R. & Frazier, A.W. (1987): X-ray powder diffraction and single-crystal data for the isomorphous series $(Fe,Al)_3(K,NH_4,H_3O)H_{14}(PO_4)_8{\cdot}4H_2O$. *Powder Diffr.,* **2**, 187-190.

Walenta, K. & Theye, T. (1999): Haigerachit, ein neues Phosphatmineral von der Grube Silberbrünnle bei Gengenbach im mittleren Schwarzwald. *Aufschluss*, **50**, 1-7.

Walenta, K. & Theye, T. (2004): $KFe^{3+3}[(H_2PO_4)_2|(HPO_4)_4]{\cdot}6H_2O$, ein zweites neues Phosphatmineral von der Grube Silberbrünnle im mittleren Schwarzwald. *Der Erzgräber*, **18**, 17-23.

Walenta, K. & Theye, T. (2005): $KFe^{3+3}[(H_2PO_4)_2|(HPO_4)_4]{\cdot}6H_2O$, ein zweites neues Phosphatmineral von der Grube Silberbrünnle im mittleren Schwarzwald. *Am. Mineral.,* **90**, 1228.

Wood, R.M. & Palenik, G.J. (1999): Bond Valence Sums in coordination chemistry using new R_0 values. Potassium-oxygen complexes. *Inorg. Chem.,* **38**, 1031-1034.

Zemann, J. (1947): The structure of pharmacosiderite. *Experientia,* **3**, 452.

Zemann, J. (1948): Formula and structural type of pharmacosiderite. *Tscher. Miner. Petrogr.,* **1**, 1-13.

Zemann, J. (1959): Isotypes between pharmacosiderite and zeolitic germanates. *Acta Crystallogr.,* **12**, 252.

Received 10 November 2006
Modified version received 22 January 2006
Accepted 12 March 2007